Solid State Science and Technology, Vol. 12, No. 1 (2004) 90-97

THE ELECTRICAL, STRUCTURAL AND THERMAL PROPERTIES OF COPPER(II) 4-AMINOBENZOATE AND COPPER(II) 3,5-DINITROBENZOATE

Richard Ritikos[a] and Siti Meriam Ab. Gani[a], Norbani Abdullah[b]

[a]*Solid State Physics Research Laboratory*
Physics Department, Universiti Malaya
50603 Kuala Lumpur
rritikos@um.edu.my, smag@um.edu.my

[b]*Chemistry Department, Universiti Malaya*
50603 Kuala Lumpur
norbania@um.edu.my

ABSTRACT

The electrical, structural and thermal properties of copper(II) 4-aminobenzoate and copper(II) 3,5-dinitrobenzoate are reported. The direct current conductivities were analyzed at low ($10 < T(K) < 300$) and at high temperatures ($300 < T(K) < 440$). The Mott's variable range hopping and Arrhenius laws were used as models for the conductivity profiles obtained. The results show that the electronic conduction characteristics of these materials depend on the structure and thermal stability. X-ray powder diffraction, infrared spectroscopy, thermogravimetric analysis and differential scanning calorimetry support the above findings.

INTRODUCTION

The electronic and metallomesogenic properties of transition metal complexes have received increasing attention in recent years, owing to the variability in both designs and practical applications offered by these materials [1,2,3]. Examples are the electron-rich bimetallic carboxylates, $M_2(O_2CR)_4$, which has a paddle-wheel or lantern structure [4]. In the solid state, each metal may be further coordinated along the M-M axis either by neutral ligand or via intermolecular interactions with its neighbors, to become powerful building blocks for 1-D coordination polymers. This paper compares the electronic properties of copper(II) 4-aminobenzoate, which has an electron-donating amino group ($-NH_2$) at the *para* position, with that of copper(II) 3,5-dinitrobenzoate, which has two electron-attracting nitro groups ($-NO_2$) at the *meta* positions [5,6]. The electronic properties of these materials are correlated with their structural and thermal properties.

EXPERIMENTAL DETAILS

Copper(II) 4-aminobenzoate (CAB) and copper(II) 3,5-dinitrobenzoate (CDNB) were prepared from copper(II) acetate monohydrate (CA) and 4-aminobenzoic acid (ABA) and 3,5-dinitrobenzoic acid (DNBA) respectively, with acetonitrile as solvent. CAB is a dark green powder while CDNB is a light blue powder. These complexes were analyzed as

potassium bromide (KBr) disc by Fourier Transform Infrared spectroscopy (FTIR). Their thermal properties were analyzed by Differential Scanning Calorimetry (DSC) and Thermal Gravimetric Analysis (TGA). The transverse direct current conductivities were measured as pellets (about 13 mm diameter and approximately 0.5 mm thickness) in the temperature range 10-440K. A cryostat with closed cycle liquid helium refrigerator was used to measure the conductivity in the temperature range 10-300K, and a heating chamber was used to measure the conductivity in the temperature range 300-440K. The x-ray diffraction (XRD) patterns were recorded using the Cu K_α line.

RESULTS AND DISCUSSION

Comparative analysis of the FTIR spectra and data for CAB, CDNB, CA and the corresponding acids show distinct differences between the starting materials and the products. The results show the presence of bonds and functional groups expected [7,8] for CAB and CDNB. These are depicted in Table 1. The values of $\nu(COO)_{asym}$ for CAB and CDNB are lower than their corresponding free acids, indicating the resonance effect of the substituents on the ligands. The values show a shift of about 43 cm^{-1} for CAB and 56 cm^{-1} for CDNB, compared to that of the corresponding free acid. The difference ($\nu(COO)_{asym}$ -$\nu(COO)_{sym}$) for CAB is 191 cm^{-1} and for CDNB is 246 cm^{-1}. The shift and the difference agree with the bridging coordination of the benzoato ligands [1,9]. The structure proposed for these materials, based on the reported structure of copper(II) benzoate [2,10] and other metal carboxylates [11,12,13], is shown in Figure 1.

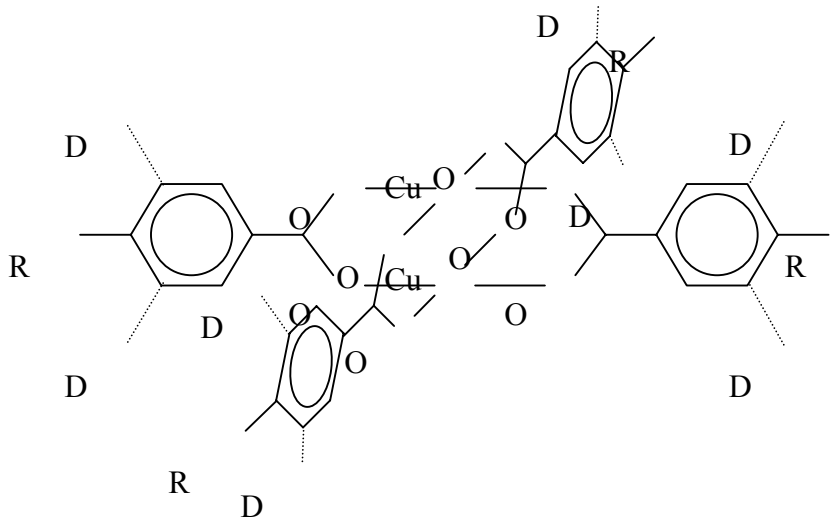

Figure 1. The proposed structure of CAB and CDNB. For CAB, R represents -NH_2 and D represents H; for CDNB, R represents H, and D represents -NO_2

Table 1. FTIR data for copper(II) acetate, copper(II) 4-aminobenzoate, copper(II) 3,5 dinitrobenzoate and their corresponding acids

Assignment	**Wavenumber / cm^{-1}**				
	CA	**ABA**	**CAB**	**DNBA**	**CDNB**
C-H aro γ_{asym}	-	3229 *w*	3213 *m*	3097 *m*	3093 *m*
C=C aro γ_{asym}	-	1636 *s,d*	1575 *s*	1630 *m*	1628 *s,b*
C=C aro γ_{sym}	-	1423 *m*	1397 *s,b*	1276 *s*	1399 *s,b*
$-COO^{-}$ γ_{asym}	1602 *s,b*	1668 *s, b*	1625 *s, d*	1701 *s,b*	1645 *s,d*
$-COO^{-}$ γ_{sym}	1445 *s,b*	1442 *m*	1434 *s*	1473 *s*	1467 *s,b*
-OH	3649-3000 *s,b*	3500-2500 *b*	-	3200-2200 *b*	-
CH_3 γ_{asym}	2989 *w*	-	-	-	-
CH_3 γ_{sym}	2942 *w*	-	-	-	-
N-H γ_{asym}	-	3460 *s,d*	3253 *m,b*	-	-
N-H γ_{sym}	-	3363 *s,d*	3140 *m,b*	-	-
N-H δ_{wag}	-	842 *s*	854 *m*	-	-
C-N γ	-	1289 *s,b*	1386 *s, b*	809 *m*	791 *m*
N-O γ_{asym}	-	-	-	1540 *s*	1538 *s*
N-O γ_{sym}	-	-	-	1346 *s*	1343 *s*
para sub.	-	770 *s*	778 *s*	-	-
1,3,5- trisub.	-	-	-	722 *s*	731 *s,d*

Aro, aromatic; γ, stretching; asym, asymmetrical; sym, symmetrical; s, sharp; m, medium; w, weak; b, broad; d, doublet

DSC patterns depicted in Figure 2 indicate that CAB does not undergo any structural changes up to 523K, while CDNB shows structural changes at approximately 420K and 434K. TGA results shows no weight lost in this temperature range for both materials. The higher stability of CAB is associated with the presence of $-NH_2$ group at the benzoato ligand, which forms interchain hydrogen bonding. Comparatively, the nitro groups in CDNB may induce a filling effect [3] which lowers its structural stability as a result of dipole-dipole repulsion. XRD analysis for CAB and CDNB show that both materials are polycrystalline. The particle size, calculated from the Scherrer equation [14], is 57 nm for CAB and 38 nm for CDNB. The larger particle size of CAB is a result of the higher structural order due to hydrogen bonding, as implied from DSC.

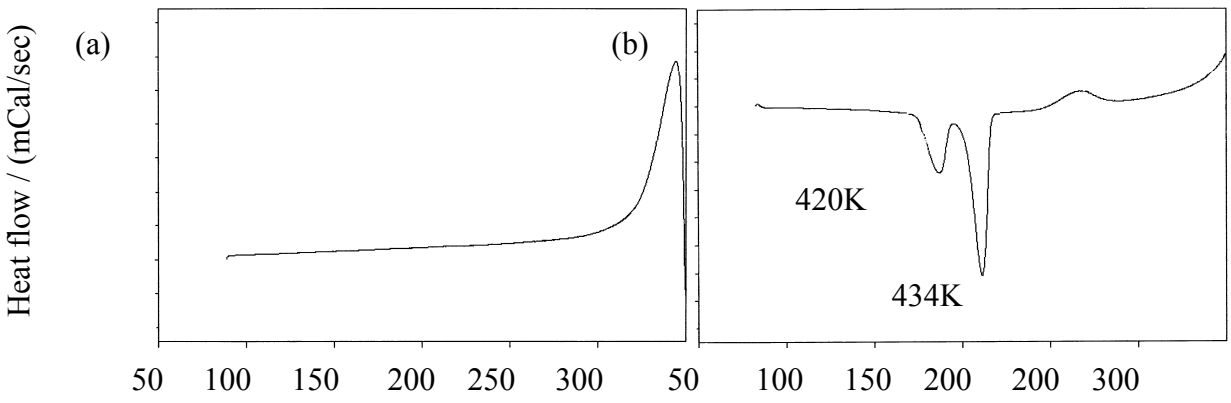

Figure 2. DSC of (a) CAB and (b) CDNB

The current-voltage characteristics of CAB and CDNB show ohmic behavior throughout the measured temperature range up to 410K. The room temperature conductivities for CAB and CDNB (Table 2) are higher than that reported for copper(II) benzoate (5.98×10^{-12} $\Omega^{-1}cm^{-1}$) [5]. This is attributed to the presence of electron donating -NH_2 and electron withdrawing -NO_2 substituents on the benzoato ligand [15]. The electronic transport for CAB and CDNB are by intrachain and interchain hopping mechanisms. The higher potential energy of interchain hopping is the limiting factor in the conductivity of these materials. The presence of electron donating –NH_2 group at the benzoato ligand for CAB is expected to increase the electron density in the ring and thus increase the intrachain conduction. On the other hand, the resulting partial positive charge on nitrogen increases the interchain distance due to dipole-dipole repulsion, which decreases the interchain conduction. [16]. The combination of these effects explained the higher conductivity of CAB compared to that of CB. The presence of two –NO_2 groups in CDNB result in a higher resonance effect on the ligand, which increases ring conjugation. This effect may explain the higher conductivity of CDNB compared to that of CAB and CB.

Figure 3 shows metal-like conduction between 10K to about 300K for CAB and CDNB. The variation of conductivity in the temperature range 300-440K for both materials is shown in Figure 4. For CDNB, the metal-insulator transition occurs at just below room temperature (286K) while for CAB it occurs at a much higher temperature (329K). This might be attributed to the relative thermal stability of both materials. We predict the premature transition for CDNB is due to the filling effect, which decreases the interchain distance and thus requires lower thermally activated energy for hopping transportation. This effect also increases the π-electron interchain delocalization in the material [17].

Within the insulating region (Figure 4), the curves are characterized by two and three activation-energy values for CAB and CDNB respectively (Table 3). The variations in activation energy with temperature suggest that the band model is not sufficient to explain the observed conductivity of both materials [18]. Such changes have been reported to be caused by changes in the mode of conduction during the heating process [15]. Furthermore, the relative stability of CAB and CDNB in this temperature range, as shown by DSC, suggests that the changes in conduction mechanism are thermally activated. It is assumed that the first step in the conduction process is essentially due to electronic conduction through the delocalization of the π-electrons which increases the hopping conduction. In the second step,

which occurs at higher temperatures for both materials, the conduction is due to the excitation of electrons from the highest occupied molecular orbital to the lowest unoccupied molecular orbital. Thus the electron is assumed to tunnel to an equivalent empty level of a neighboring molecule in the anodic direction, whereas the positive hole moves in the cathodic direction.

Table 2. Electrical conductivity and activation energies for CAB and CDNB.

CAB	**T / K**	-	329-389	393-429
	ΔE / eV	-	0.33	1.45
	σ x 10^{-11} / Scm^{-1} (296K)	6.69		
CDNB	**T / K**	282-326	330-384	403-436
	ΔE / eV	0.05	0.19	1.34
	σ x 10^{-11} / Scm^{-1} (296K)	9.07		

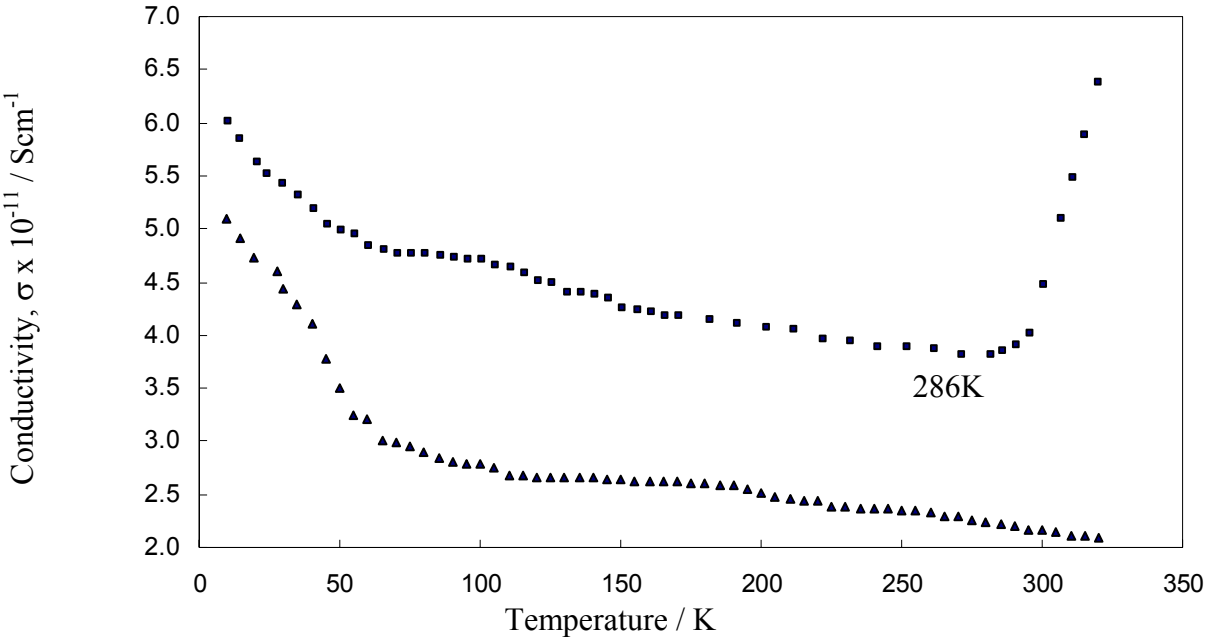

Figure 3. Variation of conductivity of CAB (▲) and CDNB (■) with temperature

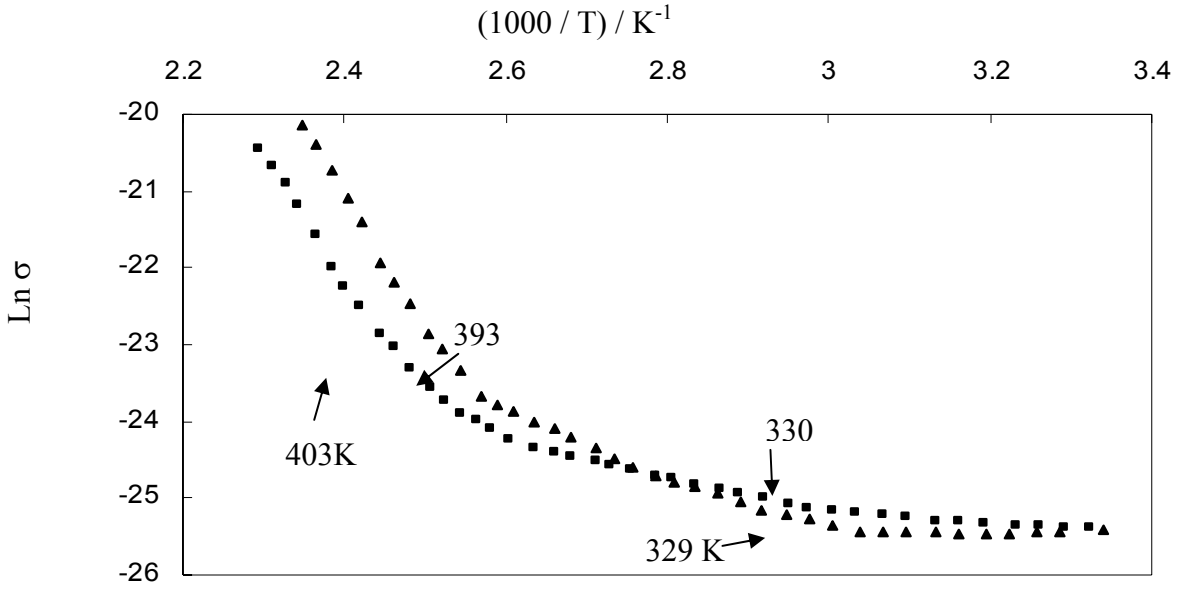

Figure 4. The variation of electrical conductivity as a function of reciprocal absolute temperature for CAB (▲) and CDNB (■)

The different conduction mechanisms at different temperature ranges for CAB are not due to structural changes. This is confirmed by the similarity of the FTIR spectra at room temperature with that at 353K and 440K. XRD spectra are similar and the particle size remains the same at these temperatures. However for CDNB, an obvious shift in peaks at 353K and 440K indicates a change of crystallinity, although the particle size remains about the same. The FTIR spectrum at room temperature is similar to that at 353K and 440K indicating that the peak shifts in XRD spectra are not due to change of structure but due to improved ordering within the same structure.

According to Mott's law [19], hopping conduction occurs in states whose energies are concentrated in a narrow band near the Fermi level. The temperature dependence of the dc conductivity for CAB and CDNB, according to Mott's VRH model in three dimension [20,21] is depicted in Figure 5. Table 3 lists the calculated values obtained based on this model. This includes Mott characteristic temperature, T_o, the density of states at Fermi level, $N(E_F)$, the density of charge carriers, n, the hopping distance, R, and hopping energy, $\Delta\varepsilon$. The values of n, R and $\Delta\varepsilon$ are calculated at specific temperatures, T.

The hopping distance, R, for CAB is larger than CDNB, which is as expected from the higher interchain distance due to hydrogen bonding for CAB and the filling effect in CDNB. However, the values of R for both materials are smaller than their particle size. This suggests two possibilities: firstly that the hopping transportation is confined within the delocalized state of the granular system, and secondly that R represents the separation between the granule in which the hopping transportation occurs. In both cases, the limiting factor would be the grain boundaries between particles. The hopping energy values appear to be similar to the activation energy calculated from the Arrhenius plot. This indicates that the activation energy values are in actual fact the result of the hopping transportation and the electrical mechanism does not comply with the band model.

$T^{-1/4}$ / $K^{-1/4}$

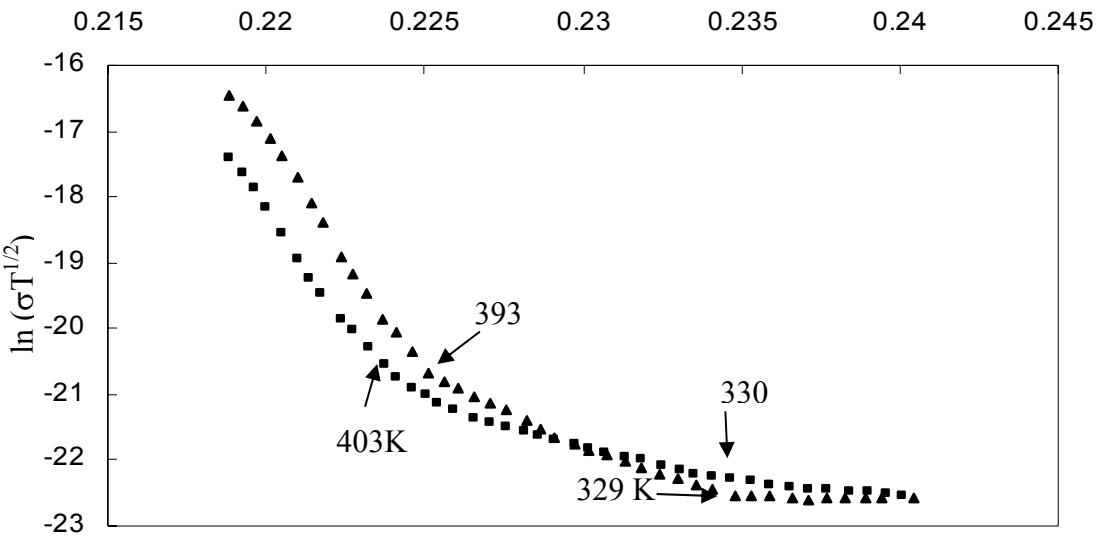

Figure 5. The 3D variable range hopping model for CAB (▲) and CDNB (■)

Table 3. Variable range hopping parameters

Properties	**CAB**		**CDNB**		
Temp. range / K	329-389	393-429	282-326	330-384	403-436
T_o / K	1.46×10^{9}	2.87×10^{11}	2.80×10^{6}	1.94×10^{8}	2.18×10^{11}
$N(E_F)$ ($eV^{-1}cm^3$)	6.65×10^{17}	3.39×10^{15}	3.47×10^{20}	5.02×10^{18}	4.47×10^{15}
T / K	353	420	300	353	420
n / cm^3	2.02×10^{16}	1.23×10^{14}	8.98×10^{18}	1.53×10^{17}	1.69×10^{14}
R / cm	1.02×10^{-6}	3.64×10^{-6}	2.21×10^{-7}	6.13×10^{-7}	3.36×10^{-6}
Δε / eV	0.34	1.46	0.06	0.21	1.41

CONCLUSION

The observed properties of CAB and CDNB are due to the differences in the intermolecular forces of attraction of the substituents on the benzoato ligand. The NH_2 group in CAB can form interchain H-bonding, while the NO_2 group in CDNB results in the filling effect. These effects influence the thermal and electronic properties of the materials. CAB is thermally more stable but CDNB has higher room temperature conductivity. The electrical transportation in both materials could be explained through Mott's VRH hopping model. Metal-insulator transition occurs at lower temperature for CDNB compared to CAB, and may be due to the relative shorter interchain distance of the former material.

REFERENCES

[1] Joaquin B., Esteruelas M.A., Levelut A.M., Oro L.A., Serrano J.L. and Sola E., *Inorg. Chem.,* **31** (1992) 732-737.

[2] Nukada R., Mori W., Takamizawa S., Mikuriya M., Handa M. and Naono H., *Chem. Lett.*, **5** (1999) 367-368.

[3] Rusjan M., Donnio B., Guillon, D., and Cukiernik F. D., *Chem. Mater.,* **14(4)** (2002) 1564-1575.

[4] Chisholm M.H., Christou G., Folting K., Huffman J.C., James C.A., Samuels J.A., Wesemann J.L. and Woodruff W.H., *Inorg. Chem.*, **35** (1996) 3643-3658.

[5] Ritikos R., Ab. Gani S.M. and Abdullah N., *J. Fiz. Mal*., **23** (2002) 97-99.

[6] Norbani Abdullah, Wan Haliza Abd. Majid, Siti Meriam Ab. Gani and Saadah Abdul Rahman, 1997. *Bulletin of Malaysian Solid State Science & Technology*, **7(2)** (1997) 43.

[7] Silverstein, R.M., *Spectrometric Identification of Organic Compounds*, Sixth Ed. John Wiley & Sons Inc. (1998) 71-109.

[8] Pavia D.L, Lampman G.M. and Kriz G.S**.,** *Introduction to Spectroscopy*, Second Ed., Saunders College Pudlishing, (1996) 14-94.

[9] Deacon G.B. and Phillips R.J., *Coord. Chem. Rev*., **33** (1980) 227-250.

[10] Kawata T., Uekusa H., Ohiba S., Furukawa T., Tokii T., Muto Y. and Kato M., *Acta Cryst.,* **B48** (1992) 253-261.

[11] Attard G.S. and Cullum P.R., *Liq. Cryst.*, **8** (1990) 299-309.

[12] Giroud-Godquin A.M., Latour J.M. and Marchon J.C., *Inorg. Chem.*, **24** (1985) 4452-4454.

[13] Douglas B., McDaniel D. and Alexander J., *Concepts and Models of Inorganic Chemistry*, John Wiley & Sons (1993).

[14] Klug H.P. and Alexander L.E., *X-ray Diffraction Procedures for Polycrystalline and Amorphous Materials*, John Wiley and Sons Inc. (1985).

[15] Mounir M., Darwish K.A., El-Ansary A.L. and Hassib H.B., *Thermochimica Acta*., **114** (1987) 257-263.

[16] Keller H.J., Low Dimensional Cooperative Phenomena, Plenum Press, New York, (1975).

[17] Wang A.H., Javadi H.S., Ray A., MacDiarmid A.G. and Epstein A.J., *Phys. Rev. B*, **42** (1990) 5411-5414.

[18] Gosh M., Barman A., Meikap A.K., De S.K. and Chatterjee S., *Phys. Lett. A*, **260** (1996) 138-148.

[19] Mott N.F., *Metal-Insulator Transitions*, Taylor & Francis Ltd (1974).

[20] Briers J., Eevers W., Cos. P., Geise H.J., Mertens R., Nagel P., Zhang X.B., Van Tendeloo G., Herrebot W. and Van der Veken B., *Polymer*, **35** (1994) 4569.

[21] Brodsky M.H., *Amorphous Semiconductors*, Springer-Verlag Berlin Heidelberg (1979).